



Ingeniería, investigación y tecnología

ISSN: 1405-7743

Facultad de Ingeniería, UNAM

Martínez-Montejano, Roberto Carlos; Castillo-Escandón, Carlos Miguel; Espinoza-López, Víctor Esteban; Campos-Cantón, Isaac; Neira-Velázquez, María Guadalupe; Soria-Arguello, Gustavo

Construction of a power electronic source for cold plasma generation

Ingeniería, investigación y tecnología, vol. XX, no. 4, 00011, 2019, October-December

Facultad de Ingeniería, UNAM

DOI: <https://doi.org/10.22201/fi.25940732e.2019.20n4.047>

Available in: <https://www.redalyc.org/articulo.oa?id=40465053011>

- How to cite
- Complete issue
- More information about this article
- Journal's webpage in redalyc.org

UNAM
redalyc.org

Scientific Information System Redalyc

Network of Scientific Journals from Latin America and the Caribbean, Spain and Portugal

Project academic non-profit, developed under the open access initiative



Construction of a power electronic source for cold plasma generation

Construcción de una fuente de electrónica de potencia para generación de plasma frío

Martínez-Montejano Roberto Carlos

Unidad Académica Multidisciplinaria Zona Media

Universidad Autónoma de San Luis Potosí

Correo: roberto.montejano@uaslp.mx

<https://orcid.org/0000-0002-8996-4134>

Castillo-Escandón Carlos Miguel

Unidad Académica Multidisciplinaria Zona Media

Universidad Autónoma de San Luis Potosí

Correo: miguel213211@yahoo.com

<https://orcid.org/0000-0001-6739-9405>

Espinoza-López Víctor Esteban

Unidad Académica Multidisciplinaria Zona Media

Universidad Autónoma de San Luis Potosí

Correo: victor.espinoza@uaslp.mx

<https://orcid.org/0000-0001-8808-2319>

Campos-Cantón Isaac

Universidad Autónoma de San Luis Potosí

Facultad de Ciencias

Correo: icampos@fciencias.uaslp.mx

<https://orcid.org/0000-0002-3189-3417>

Neira-Velázquez María Guadalupe

Departamento de Síntesis de Polímeros

Centro de Investigación en Química Aplicada

Correo: guadalupe.neira@ciqa.edu.mx

<https://orcid.org/0000-0002-3850-850X>

Soria-Arguello Gustavo

Departamento de Síntesis de Polímeros

Centro de Investigación en Química Aplicada

Correo: gustavo.soria@ciqa.edu.mx

<https://orcid.org/0000-0002-9771-8638>

Abstract

This paper presents the development of a high voltage and high-frequency power electronics source, for plasma generation, at atmospheric pressure and vacuum, using helium and air as working gases. The source design consists of an inductive (L) full bridge series resonant inverter at high frequency, where the control implemented allows varying duty cycle and frequency. Plasma generation is made by high voltage with the power signal applied on two electrodes, which provides a strong electric field that excites, and thus, ionize helium particles or air particles. The power electronic source operation was tested in different plasma reactor configurations (dielectric barrier discharge, double dielectric barrier discharge, and jet type discharge). The developed power electronics source shows a correct performance and generate a strong electric field to achieve the plasma discharges desired.

Keywords: High voltage power source, cold plasma, resonant full bridge inverter.

Resumen

Este artículo presenta el desarrollo de una fuente de electrónica de potencia de alto voltaje y alta frecuencia para la generación de plasma al vacío y a presión atmosférica, utilizando helio y aire como gases precursores. El diseño de la fuente consiste en un inversor de resonante en serie de puente completo con carga inductiva (L), que tiene un control implementado que permite variar el ciclo de trabajo y la frecuencia. La generación del plasma se logra aplicando una señal de alto voltaje en dos electrodos, que proveen un campo eléctrico fuerte que excita e ioniza partículas de helio o aire. Las descargas de plasma fueron hechas en diferentes configuraciones de electrodos: descarga de barrera dieléctrica, descarga de doble barrera dieléctrica y descarga tipo jet. La fuente de electrónica de potencia desarrollada demuestra su capacidad de desarrollar el campo eléctrico lo suficientemente fuerte para alcanzar las descargas de plasma deseadas.

Descriptores: Fuente de potencia de alto voltaje, plasma frío, inversor resonante de puente completo.

INTRODUCTION

The plasma is known as the fourth state matter, it is an ionized gas containing electric charge particles (radicals, ions, electrons, neutral atoms, molecules and other exciting species in a concentration relationship which global total electric discharge equals to zero), which maintain collective energetic interactions simultaneously. These interactions make the plasma highly reactive and can be used in wide applications through processing its control parameters. Commonly, according to its temperature, the plasma is classified into two main groups: cold plasma and thermal plasma (Tendero *et al.*, 2006; Hnautic *et al.*, 2012).

For cold plasma, the ions and neutrons temperature is near to environmental temperature and it is usually produced at low pressure (less than 1 atm) (Schutze *et al.*, 1998).

In recent years, the cold plasma has been widely used for chemical processing of water treatment, material manufacturing, semiconductor devices production, industrial disinfection, etc. The plasma generator purpose is to provide ionized species for deposition, removal, and surface preparation in the manufacturing process. The predictable, repeatable and ions characteristics are critical for the end product quality (Millner 2008; Kim *et al.*, 2006; Ren *et al.*, 2016).

There are several excitation forms to obtain cold plasma as microwave or radiofrequency systems, where operation frequency is too high and the equipment requires complex vacuum features (Wang *et al.*, 2017). Another method is by using electrical fields generated through direct current, alternating current or pulsed discharges. Intense electrical fields promote gas electrical rupture; the particles are charged and accelerated on this field, causing a partially ionized gas due to elastic collisions of these particles. The electrical fields can be produced at high voltage and high frequency (Birle *et al.*, 2011; Levchenko *et al.*, 2016).

An alternative to producing that features of electrical fields described above is by electric inverters, which are electronic circuits that produce alternant current from direct current with frequency and voltage control. Some applications of electric inverters are for supplying,

electric arc discharge or variable speed AC motor driving (Martínez *et al.*, 2014).

The aim of this work is to obtain cold plasma at atmospheric pressure and vacuum by using a high-voltage and high-frequency power electronic source in different reactors types such as jet system, dielectric barrier system, and double dielectric barrier system. The inverter objectives are to control voltage discharge, pulsated discharge time, and operation frequency for optimizing plasma generation.

The rest of the paper is organized as follows: section II presents the power electronics source development and general considerations. On section III, numerical results, experimental results, and plasma discharges on three different plasma reactors are presented. Finally, section IV concludes the paper.

POWER ELECTRONICS SOURCE DEVELOPMENT

In this section, the high voltage and high-frequency power electronics source design for non-thermal plasma is present. For this purpose, a full bridge inverter modulated by PWM is considered, as shown in Figure 1.

The general idea is to provide an AC voltage signal at high frequency and high voltage to generate an electric field, in order to make the discharge on two electrodes connected at the transformer output to obtain the non-thermal plasma. There are not exists an operation power desired each plasma reactor unique characteristics where the power applied depends on operation pressure, working gas, among others. In the literature are found a power up to 200 W or 400 W at high frequencies (Schutze *et al.*, 1998). According to the previous research, the power source is designed to operate in a wide range of powers, from 0-600 W, this allows to have control in different applications, and possibilities to use it in different plasma reactors. To achieve these characteristics, the maximum power is fixed at 600 W, and the current at 0.6 A, then the voltage is obtained by

$$V = \frac{P}{I} = \frac{600W}{0.6A} = 1000V \quad (1)$$

The design considers a boost transformer of 1:50 relation spin, then, the value provided for the input DC source it must be at least 20 V.

The topology considered for generating the AC signal is formed by four switching semiconductor devices (M1, M2, M3, M4). These devices are capable to provide positive, negative, and zero voltage to the load, by turning on and turning off as seen in Table 1.

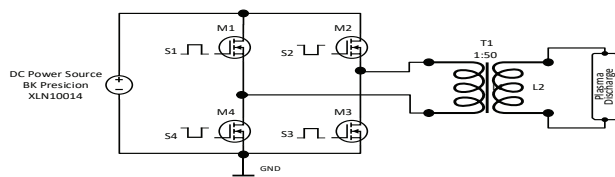


Figure 1. Full bridge inverter diagram

The output current depends on the load coupled to the inverter, the transformer primary side is considered as RLC series load, which generates a quasi-sinusoidal signal. The inverter is working as a resonant inverter, where the resonant frequency (Karys, 2009) is given by

$$\omega_0 = \frac{1}{\sqrt{LC}} \quad (2)$$

And the quality factor (Juárez *et al.*, 2016) is obtained using the following equation

$$Q = \frac{\omega_0 L}{R} \quad (3)$$

Finally, the voltage and current at the end of the transformer feed the plasma reactor, in order to provide enough energy for the plasma discharge.

INVERTER CONSTRUCTION STAGE

Three blocks are primordial on inverter construction stage, as described in the following paragraphs.

A) POWER BLOCK

The power block shown in Figure 2 in the red box is the system heart, generates a square bipolar signal from a DC signal provided by the source. It consists of an H-bridge with four transistors and a DC source. The transistors are selected according to the nominal power

(0-600 W) and the commutation frequency (0-150 kHz), so then, the MOSFET IRFP4550 is suitable for these characteristics. The DC source is given by a programmable commercial source BK PRECISION XLN10014, capable to vary its output voltage from 0 to 100 V on DC and 14.4 A. This allows to achieve the power stated on Section II.

In order to activate the power devices, it is necessary to add a circuit, to guarantee the correct voltage level from the control block, this can be achieved using a driver. This driver has three purposes: providing high impedance at the input, adapt the voltage levels, and incorporate a dead time. The selected device was the IR2110, capable to control 2 MOSFETs of the same branch. The IR2110 electric diagram the H-bridge is depicted in Figure 2 in the black box. The capacitor and resistor values are given in the datasheet, the S1 and S2 signals are obtained from TL494.

B) CONTROL BLOCK

The control block, create the signals to achieve the activation and deactivation of the power semiconductor devices, this can be accomplished by a square signal oscillator. The device selected consist in a TL494, capable to provide two pulse width modulation (PWM) signals at fixed or variable frequency. The TL494 compares a saw-tooth signal with a constant given by an internal capacitor to attain the width desired at the PWM signal, to obtain the control signals.

Table 1. Voltages levels by turning on and off the switching devices

V_{CD}	M1	M2	M3	M4
$+V_{CD}$	On	Off	On	Off
$-V_{CD}$	Off	On	Off	On
0	Off	Off	Off	Off

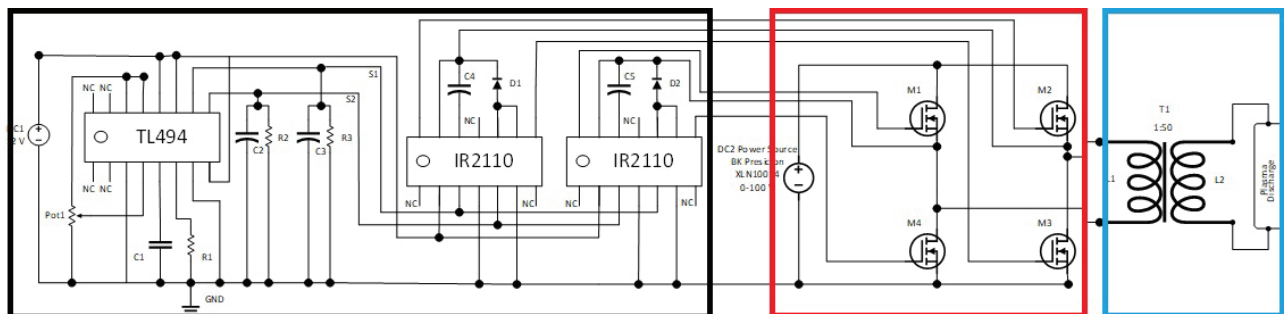


Figure 2. Full electric diagram of the proposed prototype

The TL494 is also capable to generate a dead time, consisting of a small delay at the transistor when turning on. The dead time is used to prevent short circuits, due to the MOSFETs have to work in pairs (branch) according to the electric diagram (basic inverter performance).

The frequency of the oscillator at TL494 is programmed by selecting timing components R_1 and C_1 . The TL494 internal oscillator charges the external timing capacitor with a constant current, the value of which is determined by the external timing resistor. This produces a linear-ramp voltage waveform. When the voltage across capacitor reaches 3 V, the oscillator circuit discharges it and the charging cycle is reinitiated. This oscillator frequency is equal to the TL494 output frequency. For push-pull applications the output frequency is given according to the component datasheet by

$$f_0 = (0.5) \frac{1}{R_1 C_1} \quad (4)$$

Where C_1 is fixed to $0.0001 \mu F$ and for R_1 a precision potentiometer of $0-100 k\Omega$ is used. Hence, f_0 the output frequency range goes from 5 to 150 kHz. The push-pull configuration allows to habilitate alternatively each output then output 1 goes to transistors M1 and M2 from Figure 1, and output 2 to transistors M3 and M4. The maximum duty cycle for each signal S1 and S2 is 47 %, 3 % of each signal is the dead time, this is given by the potentiometer Pot1 in Figure 2 in the black box. The greatest energy transference from BK Precision source to the power block and finally to the plasma occurs at a maximum duty cycle, if this duty cycle reduces, can generate a weakly ionized plasma, unstable, and without enough energy to light it. The electric diagram of the control block is given in Figure 2 in the black box. Capacitors and resistors values are obtained from the datasheet component. Besides, the source DC1 is a commercial source BK PRECISION 9104 which operates from 0–10 V and 0–10 A. It is fixed to 12 V, and the objective of this source is to provide energy to the control block and the drivers IR2110.

C) TRANSFORMATION BLOCK

This block leads the AC signal coming from the power block to the level required for supply the load. For this purpose, a step up transformer is used, capable to manage the power of 1 kW and the spin relationship of 1:50, this is shown in the ideal form in Figure 2 at the blue box. The resistance and capacitance values at the primary of the transformer are physically measured using a BK PRECISION Bench LCR/ESR 889B from the step-up transformer, in order to obtain more accurate results. The resistance, inductance, and capacitance on the transformer primary side are 0.470Ω , $37.9 \mu H$ and $150 nF$ respectively. These values are used on equations (2) and (3), to obtain the series H-Bridge resonant circuit parameters, with a quality factor of 33.81 and a resonant frequency of 66.75 kHz. The block diagram of the proposed prototype is depicted in Figure 3.

POWER ELECTRONICS SOURCE RESULTS

A) SIMULATION RESULTS

In order to validate the proposed circuit, the numerical simulation of the power electronics source using Pspice 8.0 was carried out. The DC voltage is fixed at 30 V, the commutation signals have a 65 kHz frequency, as the load on the transformer secondary side a $50 k\Omega$ resistor is used only to verify the system performance. Figure 4 shows the simulated circuit. The circuits at the bottom of the figure simulate the PWM obtained from TL494 circuit, due to, the Pspice does not have the libraries for the TL494 and the drivers IR2110. In the transformer, the parasite values (obtained with a BK PRECISION Bench LCR/ESR 889B) are included for having more accurate results. The R3 resistor simulates an isolated ground given by transformer isolation, due to its high value does not affect the simulation.

Then, in Figure 5, the output voltage and output current at the transformer primary is depicted. The square signal represents the voltage (black color) and the quasi-sinusoidal the current signal (blue color).

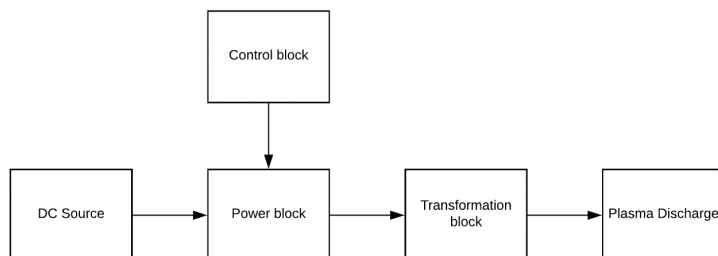


Figure 3. Block diagram of the proposed prototype

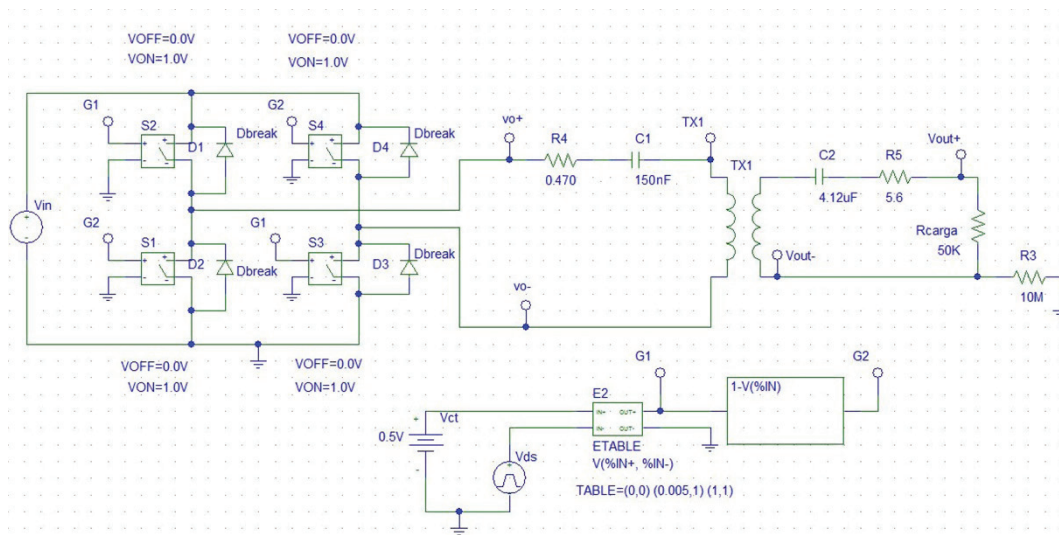


Figure 4. Full-bridge inverter developed on Pspice 8.0

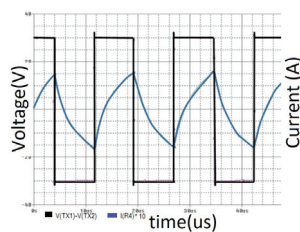


Figure 5. Voltage and current output waveforms

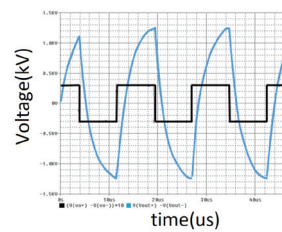


Figure 6. Inverter output voltage and voltage on the load

The square signal corresponds to the inverter output, obtaining -30 V to 30 V , and the current is quasi-sinusoidal and has different phase because of the load. The current has a different scale, its real value is of 0.7 A , it presents at the same graphic to appreciate the output waveforms.

Afterward, the voltage on the load and inverter output voltage is shown in Figure 6. The square signal corresponds to the transformer primary signal (black color) and the quasi-sinusoidal signal to the transformer secondary (blue color).

The results obtained prove the correct performance of the power supply, giving the desired power, enough to generate plasma. The signal before passing the transformer is a square signal of -30 V to 30 V at 65 kHz , and after the transformer, the signal becomes quasi-sinusoidal of 1.3 kV , due to the parasites values.

B) POWER SOURCE CONSTRUCTION

The power electronics source was built following the characteristics described in section two of this docu-

ment. Figure 7 shows the full-bridge inverter prototype, corresponding to the power block and the control block.

Then, Figure 8 depicts the experimental setup, with the DC source and the elevator transformer connected to the full-bridge inverter.

C) EXPERIMENTAL RESULTS

The experimental setup previously described was configured with the next values: the DC source was fixed at 40 V , and the switching frequency at 65 kHz . The voltage output and the current output at the primary of the transformer are shown in Figure 9. The current is the quasi-sinusoidal signal and the voltage corresponds to a square signal.

The results are consisting according to the figure 4, the inverter has a square output of -40 to 40 V and the current is quasi-sinusoidal of 0.6 A of amplitude due to the load and have a different phase.

Then, Figure 10 depicts the voltage at the inverter output as a square signal and the output voltage at the

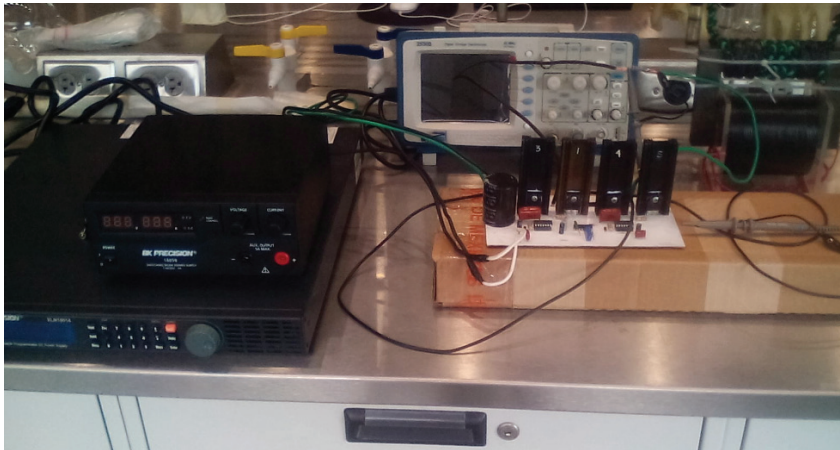


Figure 7. Full-bridge inverter prototype

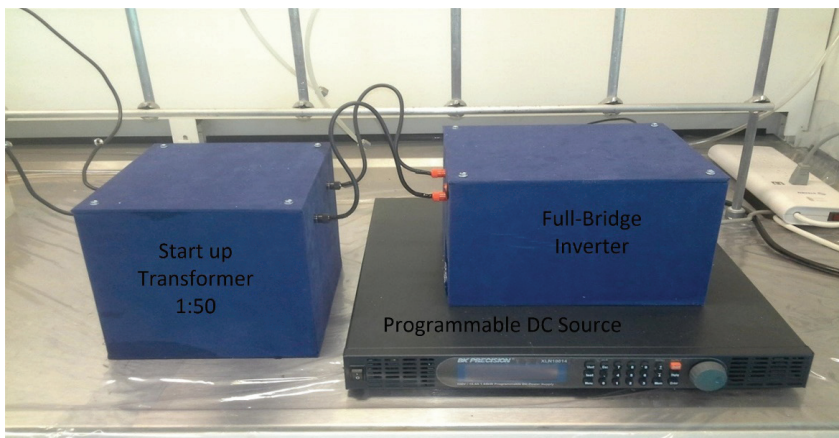


Figure 8. Experimental setup

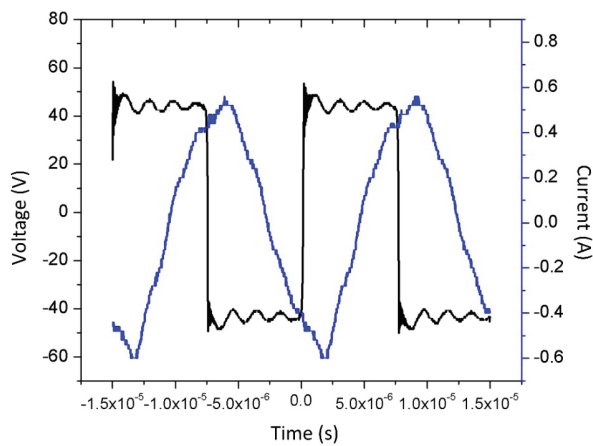


Figure 9. Inverter voltage and current output

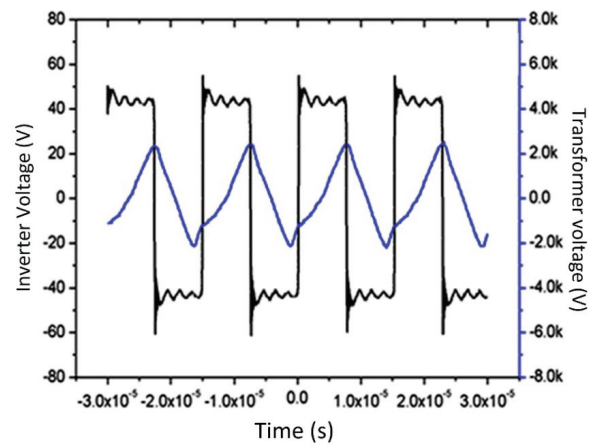


Figure 10. Voltages at the inverter and transformer outputs

Table 2. Comparative between simulation and experimental results

Parameter	Simulation	Experimental
Frequency	65 kHz	65 kHz
Voltage input	30 V	40 V
Current	0.7 A	0.6 A
Voltage at transformer output	1.3 kV	2 kV

secondary as a sinusoidal signal, with a high voltage and high frequency. These results are consistent with the simulation results in waveform and amplitude. This guarantee enough energy power to realize the plasma discharge.

A comparative table is shown in Table 2, to present the coherency between the results obtained by simulation and experimental results, the inverter output voltage is multiplied by a factor of 50 due to the transformer.

D) PLASMA DISCHARGES

For proving the power electronic source in plasma generation, different plasma reactor configurations were carried out, where the equipment was inside a cabinet built with isolate material. Besides, the circuits have a ground connection for electric discharge. The user has to wear glasses, industrial boots, and dielectric gloves for high voltage.

D.1) DIELECTRIC BARRIER DISCHARGE

Among atmospheric pressure plasma produced in several ways, the dielectric barrier discharge is mainly characterized by the use of one or more dielectrics disposed between the electrodes. This configuration produces random multifilament micro-discharges. A high-frequency electric field is required for this purposes. The dielectric barrier distributes the micro discharge uniformly throughout the discharge volume, generating energetic electrons that create other active species (Jiang *et al.*, 2018; Li *et al.*, 2018). The diagram is depicted in Figure 11.

Using the experimental setup described above, coupled with the proposed configuration, and Helium as plasma gas, the discharge showed in Figure 12, is obtained.

The dielectric used was a 20 cm long inert quartz circular tube, with 1.5 cm of diameter with two aluminum electrodes of 3 cm length and gap of 2 cm, the helium provided was regulated using a needle valve. The dielectric barrier discharges applications are well known

as etching, cleaning, thin films deposition, plasma polymerization, surface treatment, materials functionalization, and modification, etc.

D.2) DOUBLES DIELECTRIC BARRIER DISCHARGE

The double DBD plasma is provided through a double cylindrical dielectric barrier. This arrangement is useful to prevent arcing between the (inner) powered electrode and a plasma exposed sample which is particularly unwanted for general applications (Florian *et al.*, 2015; Zhang *et al.*, 2018). The Double dielectric reactor diagram is shown in Figure 13 the purple color indicates the plasma generated.

Then, Figure 14 shows a superior view of de Double dielectric reactor diagram, for better understanding of the configuration. The orange color denotes the ground electrode, the gray color the two dielectric barriers, and the black color the high voltage electrode.

The double barrier dielectric reactor operation was created, on the coaxial configuration with quartz walls with central and external electrodes. The discharges are operating in a 5 kHz to 150 kHz range, so the operating frequency was settled at 65 kHz (resonant frequency). The plasma gas was helium. Figure 15, shows the double dielectric discharge ionizing helium using the prototype developed. Dielectric material presence between both electrodes requires high AC voltages applied in a 1.2 kVp to 12 kVp, and currents from 20 to 100 mA. The power applied goes from 200 W to 1.2 kW.

D.3) JET DISCHARGE

One of the cold atmospheric plasma sources is jet type, which can generate plasmas in open space rather than in confined discharge gaps and it is characterized by flexibility, compactness, and efficiency (Fan *et al.*, 2012). The Jet plasma reactor diagram is depicted in Figure 16.

In order to produce discharges without electric arcs, a jet plasma reactor was built, for high voltage dischar-

ges at 15 kVp and operation frequencies for 5 to 150 kHz. On jet plasma discharge a shining on the reactor extreme is produced. This shining is used for material treatment and modifying the material structure. The

plasma generation was configured under parameters shown in Table 2.

With the parameters stated above, the plasma discharge obtained on a jet type reactor is shown in Figure 17, at atmospheric pressure.

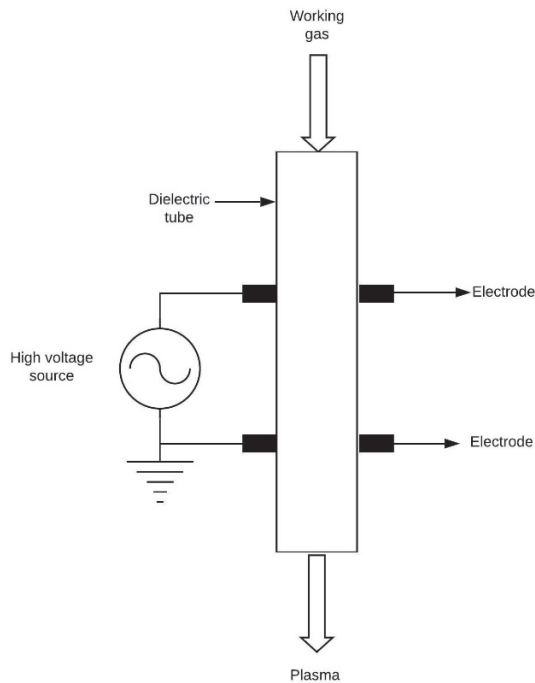


Figure 11. Dielectric plasma reactor diagram

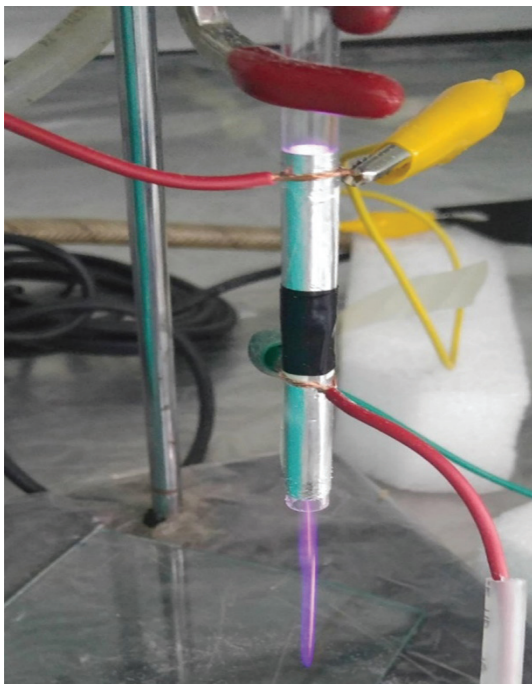


Figure 12. Dielectric barrier discharge

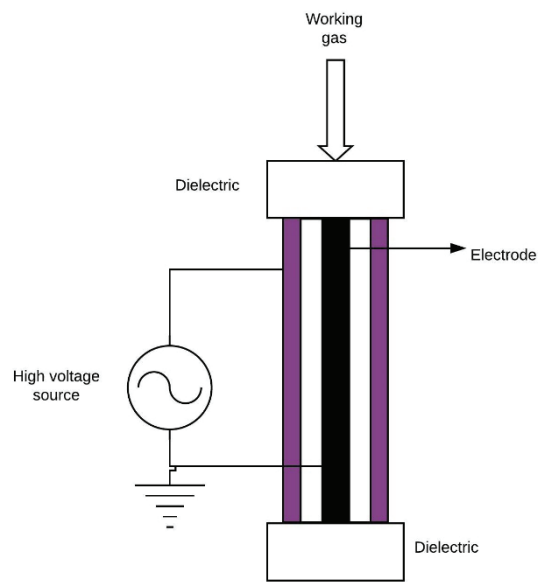


Figure 13. Double dielectric plasma reactor diagram

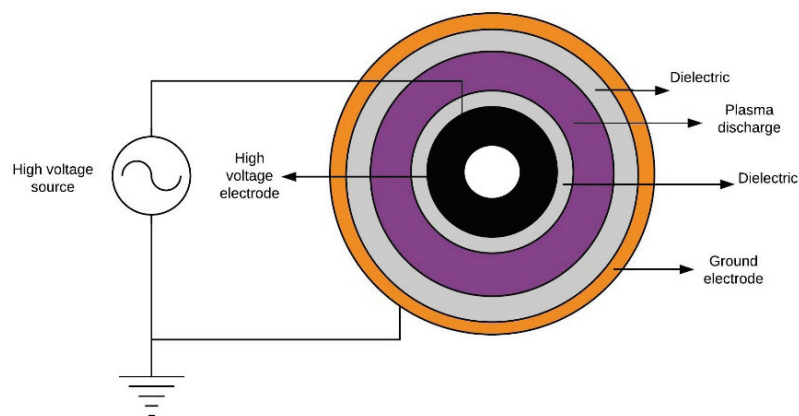


Figure 14. Superior view of double dielectric reactor diagram



Figure 15. Double dielectric barrier discharge

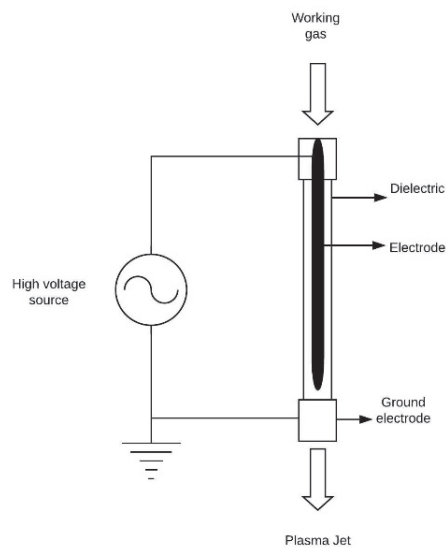


Figure 16. Jet type plasma reactor diagram

Table 3. Jet reactor parameters

Voltage	15 kVp
Current	20 mA
Power	300 W
Plasma global temperature	< 70 °C
Plasma gas	Air
Air flux	6 LPM

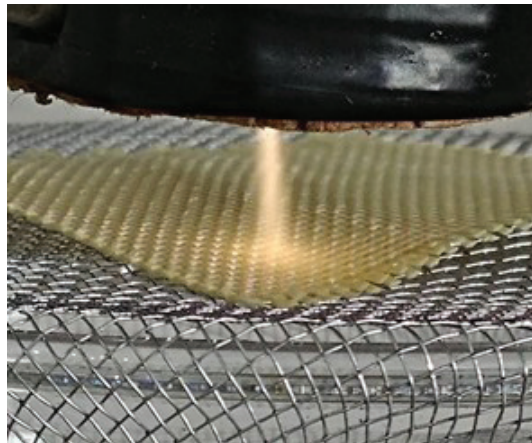


Figure 17. Plasma jet discharge ionizing air

CONCLUSIONS

The power electronic source developed allow varying the operating frequency from 5 kHz to 150 kHz, and a duty cycle from 0 to 47 %. It is coupled to a BK PRECISION XLN10014 programmable DC source, and a general purpose star up transformer to provide until 15 kVp at 1.4 kW of power. The variable frequency allows to syntonizer the natural resonance zone, and it is important because the regions of maximum voltage amplification aids to ignite and generate stable plasma discharges.

The experimental prototype design was first tested by numerical simulations and then it was built physically, the results in both, simulation and physical are consistent and coherent.

The designed prototype is useful to generate plasma discharges, which can help to modify materials, in order to enhance electrical, mechanical, and thermal properties. The proposed prototype has an electronic control that allows varying some parameters like frequency, and duty cycle, this are some advantages against plasma generation through radiofrequency, and microwave.

Plasma discharges were made for ionizing helium on two different reactor configurations: dielectric barrier, double dielectric barrier, and ionizing air on a jet type reactor. In all of them, it was possible to achieve an electrical field strong enough to reach the breakdown voltage and generate plasma discharge.

The system advantage presented in this work against other high voltage source for plasma generation, is the versatility to generate plasma at vacuum and atmosphere pressure, with electrodes on direct contact to the plasma or through dielectric discharges.

As future work is proposed to implement a feedback nonlinear control as sliding mode control or fuzzy control, to improve the prototype features, the system is in open loop, and also taste the plasma generated to modify materials.

ACKNOWLEDGEMENTS

This work was partially supported by CONACYT through the Ciencia Básica grant No. 288682 under the direction of Ku-Herrera J.J. and in part by grant 299092 Laboratorio Nacional en Innovación y Desarrollo de Materiales Ligeros para la Industria Automotriz (LANIAUTO). The authors would like to thank Sierra U., Méndez G., Lozada M. and Mercado A. for their invaluable technical support.

REFERENCES

- Birle M., Leu C. & Bauer S. (2011). Design and application of a high-frequency high-voltage generator. On Internations Symposium on High Voltage.
- Fan Q.Q., Qian M.Y., Ren C.S., Wang D. & Wen X. (2012). Discharge characteristics of a cold-atmospheric-plasma jet array generated with single electrode configuration. *IEEE Transactions on Plasma Science*, 40 (6), 1724-1729. <https://doi.org/10.1109/TPS.2012.2191307>
- Florian J., Merbahi N., Florian J., Merbahi N., Wattieaux G., Plewa J.M. & Yousfi M. (2015). Comparative studies of double dielectric barrier discharge and microwave argon plasma jets at atmospheric pressure for biomedical applications. *IEEE Transactions on Plasma Science*, 43 (9), 3332-3338. <https://doi.org/10.1109/TPS.2015.2404879>
- Hnautic E., Astanei D., Ursache M. & Hnautic B. (2012). A review over the cold plasma reactors and their applications. On 2012 International Conference and Exposition on Electrical and Power Engineering (EPE 2012), IEEE, 497-502. Retrieved from <https://doi.org/10.1109/ICEPE.2012.6463884>
- Jiang H., Shao T., Zhang C., Yiang P. & Liu H. (2018). Two typical charge transportation characteristics in nanosecond-pulse surface dielectric barrier discharge. *IEEE Transactions on Plasma Science*, 46(10), 3524-3530. <https://doi.org/10.1109/TPS.2018.2811728>
- Juárez M.A., Vázquez G., Sosa J.M., Martínez P.R. & García F. (2016). Analysis and design of resonant inverter for ozone generation. On 2016 IEEE International Autumn Meeting on Power, Electronics and Computing (ROPEC). Retrieved from <https://doi.org/10.1109/ROPEC.2016.7830644>
- Karys S. (2009). Selection of resonant circuit elements for the ARCP inverter. On 2009 10th International Conference on Electrical Power Quality and Utilisation. Retrieved from <https://doi.org/10.1109/EPQU.2009.5318855>
- Kim Y.M., Kim J.Y., Jo M.C., Lee S.H., Mun S.P., Lee H.W., Kwon S.K. & Sun K.Y. (2006). Resonance inverter power system for improving plasma sterilization effect. On 2006 CES/IEEE 5th International Power Electronics Conference. Retrieved from <https://doi.org/10.1109/IPEMC.2006.4778248>
- Levchenko I., Cvelbar U. & Keidar M. (2016). Graphene flakes in arc plasma: conditions for the fast single-layer growth. *Graphene*, 5(2), 81-89. <https://doi.org/10.4236/graphene.2016.52009>
- Li X., Chu J., Jia P., Li Y., Wang B. & Dong L. (2018). Characterization of a laminar plasma plume based on dielectric-barrier discharge at atmospheric pressure. *IEEE Transactions on Plasma Science*, 46 (3), 583-586. <https://doi.org/10.1109/TPS.2018.2797954>
- Martínez-Montejano R.C., Castillo-Meraz R., Campos-Cantón I. & Martínez-Montejano M.F. (2014). Generalization of a model based controller for the n-level cascaded H-Bridge Multilevel converter used as a shunt active filter. *International Review of Electrical Engineering*, 9 (3), 486-492.

- Millner A.R. (2008). Power electronic topologies for plasma generator. On 2008 International Symposium on Industrial Electronics, 359-362. Retrieved from <https://doi.org/10.1109/ISIE.2008.4676925>
- Ren F., Ji S., Hao Z. & Shi Y. (2016). Study of the characteristics of cold air atmospheric pressure plasma jet generated with inverted tapered tube. *IEEE Transactions on Plasma Science*, 44 (11), 2594-2602. <https://doi.org/10.1109/TPS.2016.2598418>
- Schutze A., Jeong J.Y., Babaya S.E., Park J., Selwyb G.S. & Hicks R.F. (1998). The atmospheric-pressure plasma jet: a review and comparison on the other plasma sources. *IEEE Transactions on Plasma Science*, 26(6), 1685-1694. <https://doi.org/10.1109/27.747887>
- Tendero C., Tixier C., Tristant P., Desmaison J. & Leprince P. (2006). Atmospheric pressure plasmas: A review. *Spectrochimica Acta-Part B: Atomic Spectroscopy, Elsevier*, 61 (1), 2-30. <https://doi.org/10.1016/j.sab.2005.10.003>
- Wang K., Xu M., Gu Y., Gu Z., Liu J. & Fan Q.H. (2017). Low temperature plasma exfoliated n-doped Graphene for symmetrical electrode supercapacitors. *Nano Energy, Elsevier*, 31, 486-494. <https://doi.org/10.1016/j.nanoen.2016.11.007>
- Zhang X., Xiao H., Hu X. & Zhang Y. (2018). Effects of reduced electric field on sulfur hexafluoride removal for a double dielectric barrier discharge reactor *IEEE Transactions on Plasma Science*, 46(3), 563-570. <https://doi.org/10.1109/TPS.2018.2796134>